Spectrum Sharing between Earth Exploration Satellite and Commercial Services: An Economic Feasibility Analysis

Jonathan Chamberlain
ECE Department
Boston University
Boston, Massachusetts
jdchambo@bu.edu

Joel T. Johnson
ECE Department
The Ohio State University
Columbus, Ohio
johnson.1374@osu.edu

David Starobinski
ECE Department
Boston University
Boston, Massachusetts
staro@bu.edu

***Abstract*—Microwave radiometers operating on Earth-observing satellites provide critical support for weather forecasting as well as oceanographic, atmospheric, and geophysical monitoring. Maintaining spectrum access is vital for continued support of these observations which are easily corrupted by any anthropogenic transmissions occurring within the time-frequency space utilized by the radiometers. Despite these requirements, spectrum sharing is also well motivated to accommodate the ongoing expansion of high band 5G systems, given the relative sparsity in time of radiometer spectrum access at a specific location. In this paper, we propose a joint queuing and game-theoretic model to evaluate the conditions under which commercial users have incentive to utilize shared spectrum in the face of preemptions by EESS users. The model is justified using real traces of EESS Spectrum access. We assume that commercial users are served by a provider that charges an admission fee. We determine that in such a scenario, the resulting Nash Equilibrium is unique. However, increasing the fraction of commercial users opting to utilize available spectrum lowers the incentive for newly arriving users to follow suit, impacting provider profits from admission fees. Furthermore, we show that the socially optimal state is attained with the profit-maximizing fee. These results demonstrate the potential for temporal sharing between space-based Earth observing microwave radiometers and commercial users in a manner that provides societal benefits.**

***Index Terms*—Spectrum co-existence, passive users, network economics, game theory, queuing theory.**

I. Introduction

Microwave radiometers operating on Earth-observing satellites provide measurements that are crucial for supporting high impact applications, such as weather forecasting; monitoring the oceans, atmosphere, land surface, and cryosphere; and for understanding Earth's geophysical processes [1]. The signals observed by microwave radiometers are naturally-generated thermal noise in the microwave portion of the spectrum, and the desired information on geophysical processes is obtained only if the observed thermal noise power (reported as a "brightness temperature") can be measured to a precision approaching one part in 10^3 or better. Multiple emerging scientific and operational applications are resulting in demands for even higher precision in the geophysical products obtained, due to the importance of understanding the evolution of our changing planet and the impact on human activities on these changes. Because the geophysical precision achieved is determined by the time-bandwidth product of the spectrum used in a microwave radiometer's measurement, maintaining and expanding spectrum access is crucial for supporting and improving continued and future measurements.

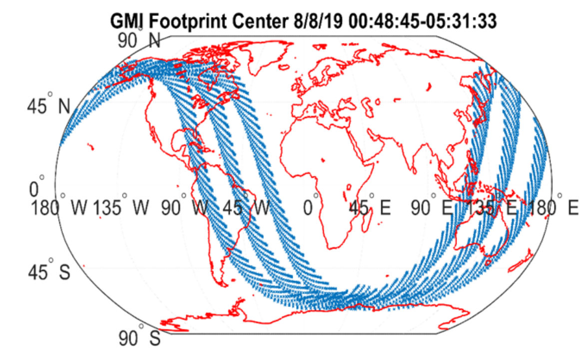

Fig. 1: Footprint locations for the GMI radiometer over an example approximate 5 hour period.

Unfortunately, microwave radiometric measurements are easily corrupted by any anthropogenic transmissions that occur in the portion of time-frequency space used by the radiometer; these transmissions are described as "radio frequency interference" (RFI) to the microwave radiometer. The importance of RFI-free observations has been recognized in past spectrum allocation activities that have granted a primary or secondary allocation for the passive *Earth Exploration Satellite-Service (EESS)* [2]. As use of these bands for other applications has continued to increase, the utility of secondary allocations is being compromised, motivating new strategies for ensuring future spectrum access. The recent concerns over RFI from "high band" 5G systems to water vapor observing microwave radiometers operating near 23 GHz [3], [4] provide clear evidence of the challenges with traditional spectrum allocation processes.

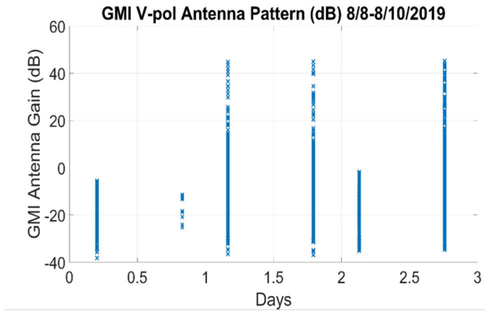

Fig. 2: Time history of GMI vertical polarization antenna gain at Columbus, OH over a selected 3 day period.

The potential for cooperative sharing within existing secondary allocations or other non-allocated bands is evident when it is considered that a spaceborne microwave radiometer observes a given location only for a small percentage of the time (e.g. during a satellite overpass). As an example of these properties, the upper left plot of Figure 1 displays "footprint" locations (i.e. the location on the Earth's surface that is being observed at one instant of time) over an approximate 5 hour period on August 8th, 2019 for the Global Microwave Imager instrument (GMI, [5]). The approximate 94 minute period of a single orbit typical for low Earth orbiting satellites is evident, as well as the wide distribution of observations in space over a relatively short time period. The temporal aspects of radiometer access are further explored in Figure 2, which illustrates GMI antenna gains directed at Columbus, OH over a 3 day period. It is noted that the access needs captured in Figure 2 represent only a single satellite radiometer system among many such systems.

Whether considered in bands currently allocated to EESS applications on a secondary basis, to bands not currently available for EESS observations, or as part of future more dynamic spectrum allocation approaches, the sparse temporal access needs of passive EESS users motivates a spectrum co-existence framework whereby these users are granted access that preempts transmissions by active commercial users. This implies that whenever EESS users need access to a spectrum band, commercial users must vacate that band. To assess the viability of such a co-existence framework, this paper analyzes its potential impact on the behavior of commercial participants, including the provider of commercial services and its users.

Because commercial users are strategic and non-cooperative in nature, game theory is the methodology of choice to analyze interactions between these participants (also known as *players* in the jargon of game theory). In this context, our objective is to characterize the equilibrium outcomes of the game (i.e., the *Nash equilibria*), as well as the resulting provider's profit and the efficiency of said equilibria. The well-established concept of *social welfare* can be used to measure this efficiency. An important goal is to evaluate how the social welfare at equilibrium fares with respect to to the *Pareto optimum*: namely, the optimal social welfare that could be achieved under a (hypothetical) centralized allocation of resources. Ideally, the social welfare at equilibrium should be as close as possible to the Pareto optimum (the ratio between the latter and the former is known as *Price of Anarchy (PoA)* [6]). The main contributions of this paper in this context can be summarized as follows:

1) We propose a framework for spectrum sharing between passive EESS users and active commercial users, relying on priority-based preemptions.
2) We introduce economics underpinnings for this framework using a joint queuing-theoretic and game-theoretic formulation. Spectrum access by commercial users (aka *customers*) is modeled using an $M/G/1$ queuing system with server breakdowns (i.e., when EESS users are using the spectrum, the server is "broken"). Strategic customers decide whether or not to join the system considering the reward of service, the cost of delay, the cost of preemptions, and the provider's admission fee.
3) We justify the model using real traces of spectrum access from a collection of EESS satellites (these traces were assembled from public sources and will be made available to the broader research community).
4) We perform an equilibrium analysis of this model, proving the existence of a unique Nash Equilibrium, and providing a closed-form expression for it.
5) We analyze the profit maximization, social welfare and PoA of this system, as a function of the various statistical traffic parameters and the economic costs. The analysis shows that the profit maximization and social welfare optimization objectives coincide for fixed queuing parameters. Therefore, it is not necessary for a regulatory body to intervene to force a socially optimal outcome.
6) Through numerical analysis, we evaluate the impact of the delay cost, the preemption cost, and EESS spectrum usage on the behavior of customers and on the provider's profit. Under typical parameters, we find that delay has greater impact than preemption on the customers' behavior and the resulting provider's profit.

II. Related Work

The economic analysis conducted in this paper relates to the field of *queuing games*, which combines queuing and game theory. The book by Hassin and Haviv is a standard reference in this field [7]. A survey of more recent results can be found in [8]. Within the field of queuing games, priority queues have been treated extensively. Most of the related literature assumes a non-preemptive service policy, whereby a low priority in service cannot be preempted by a higher priority customer. In contrast, our paper considers a preemptive-resume service policy, whereby a low-priority customer in service may be preempted by a higher priority customer (in our case, an EESS user). Prior research shows that preemptive service may lead to markedly different equilibrium outcomes than non-preemptive service [9], [10].

To model spectrum disruption by higher priority users, our work considers a specialized $M/G/1$ queuing model, namely

Parameter	Definition
λ, λ_{ee}	Arrival rate of customers and passive EESS users, respectively.
μ, μ_{ee}	Service rate of customers and EESS users, respectively (equal to 1 over mean service length).
μ'	The effective service rate of customers once service breakdowns are accounted for.
ρ'	The effective traffic load of customers (equal to arrival rate over effective service rate).
K, K_{ee}	Service variance parameter, where the second moment of service equals K/μ^2 K_{ee}/μ_{ee}^2 respectively for customers, EESS users.
C_d	Cost of customer delay in the system per time unit.
C_p	Cost of each preemption of a customer by an EESS user.
R	Customer's reward of getting service.
Q	Customer queuing utility, that is the reward of service minus the average costs due to delay and preemption.
f	Provider's admission fee.
ϕ	Fraction of customers joining the system.
ϕ^*	Mixed equilibrium.
ϕ^{max}	Equilibrium corresponding to profit-maximizing fee.
D	Random variable representing the total system delay for customers joining the system.
$\mathcal{P}$	Average provider's profit per time unit.
α, β	Respectively, $\alpha \triangleq \lambda_{ee} + \mu_{ee}$, and $\beta \triangleq 2\lambda_{ee}^2 + K_{ee}\lambda_{ee}\mu + 4\lambda_{ee}\mu_{ee} + 2\mu_{ee}^2$

TABLE I: Definition of parameters and variables related to the queuing game model. Note that ϕ^*, ϕ^{max}, D, Q and $\mathcal{P}$ are outcome variables determined by the analysis. The fee f is a parameter set by the provider. The variables α, β are notational shorthands for certain repeating expressions. The other parameters are exogenous variables.

an $M/G/1$ queue with server breakdowns. The work by Avi-Yitzhak and Naor introduces and analyzes several variants of this model [11]. One variant (referred to as Model B in [11]) assumes that breakdowns occur only when the server is busy. This also corresponds to the model analyzed in the probability textbook of Ross [12, p. 531], which was adopted in previous work on economic analysis of cognitive radios [13]. Since breakdowns cannot occur when the system is empty, this means that an arriving customer finding the system empty will get served immediately. This model does not accurately reflect spectrum sharing. In practice, a commercial user arriving while an EESS user is using the spectrum should not be allowed to access the spectrum immediately, even if it finds the system empty (i.e., no other commercial user is present).

Another variant, corresponding to *Model A* in [11], considers breakdowns that occur homogeneously in time. In other words, server breakdowns are independent of customer arrivals to the queue. This model better reflects reality, since in practice the on-off process characterizing EESS spectrum usage is independent of arrivals of commercial users to the system. In this paper, we adopt this variant. As a result, the economic analysis differs from prior work [13]. Additionally, our economic model explicitly captures the economic cost caused by preemptions, which is typically ignored in prior work.

The sharing framework considered in this paper resembles that of Citizens Broadband Radio Service (CBRS) [14] in that EESS-passive users will be considered as incumbents empowered with *preemptive priority*. This implies that whenever EESS users need access to a certain spectrum band, commercial users must vacate that band. To manage access and enforce the appropriate priority of the various users, we envision a Spectrum Access System (SAS) to monitor the spectrum space and communicate the availability of a requested channel to transmit. Eichen discusses the feasibility and practical considerations in building such a CBRS-like framework for sharing the spectrum between passive scientific users and active users [15]. Our work contributes theoretical foundations to reason about such a spectrum sharing framework. Our model evaluates the impact of service interruptions on the delay performance and strategic choices of commercial users, and the effect of such choices on the profit of a commercial provider and the social welfare of the system. A key and unique contribution of our paper consists of the validation of the statistical models with actual time series of spectrum access by EESS satellites.

III. Economic Model

In this section, we present our economic model, including the game-theoretic formulation. Table I summarizes the notation of our model.

A. Spectrum Usage Model and Customer Delay Analysis

We start by introducing a statistical model that accounts for the spectrum usage of EESS users and commercial users (we refer to the latter simply as *customers*). We assume that customers wait in a queue for service, hence our model incorporates a queuing-theoretic component.

Usage of the spectrum by the EESS users represents an *on-off process*. In the on-state, spectrum is available to customers for an exponentially distributed amount of time with rate parameter λ_{ee}. During this time, the server of the queuing system is working, and customers are served in a First-Come First-Served (FCFS) order. In the off-state, EESS users are using the spectrum. During this time, the server of the queuing system is broken (and getting repaired), and no customer is getting served. The distribution of the repair time is *general* with mean $1/\mu_{ee}$ and second moment K_{ee}/μ_{ee}^2. Once the spectrum is again available, if a customer was preempted it reenters from the point of interruption (corresponding to a preemptive-resume model [16, p. 67]).

Customers arrive to the system according to a Poisson process with rate λ. The work of Willkomm *et al.* [17] justifies the Poisson process assumption for arrivals of customers, based on measurements of spectrum usage in cellular networks. Due to the costs associated with delay and preeemption and the provider's admission fee, only a fraction $0 \leq \phi \leq 1$ of the customers join the queue. The value of ϕ is determined as the solution of a queuing game. This game is discussed in detail in Sections III-C and IV. The distribution of the spectrum usage time by each customer follows a *general* distribution with mean $1/\mu$ and second moment K/μ^2.

Since server breakdowns occur independently of customer arrivals, the system under consideration is modeled as an $M/G/1$ queue with server breakdowns occurring homogeneously in time (*Model A* in [11]).

The solution of the model in question is equivalent to a queue with the following modified parameters. Let X' represent the service time. The mean service time is $\mathbb{E}[X'] = 1/\mu'^2$ where

$$\mu' = \frac{\mu}{1 + \lambda_{ee}/\mu_{ee}}. \quad (1)$$

The resulting effective traffic load is $\rho' = \lambda\phi/\mu'$ and the system is stable if and only if $\rho' < 1$. The formula for the delay of a customer in the system is [11]:

$$\mathbb{E}[D] = \frac{(K_{ee}/\mu_{ee})(1 - \mu'/\mu) + \lambda\phi K(1/\mu'^2)}{2(1 - \rho')} + \frac{1}{\mu'}. \quad (2)$$

The first term in Eq. (2) represents the delay of a customer in the queue (also known as *waiting time* in the literature on queuing theory). We note that even when $\lambda \to 0$ the waiting time does not vanish; that is, even if the customers' demand is very low, a customer may have to wait upon arrival due to the spectrum currently being held by an EESS user. The second term represents the effective mean service time of a customer. This quantity is greater than $1/\mu$ because a customer may be preempted by an EESS user while being served. Specifically, because EESS users hold the spectrum for the following fraction of time

$$\frac{1/\mu_{ee}}{1/\mu_{ee} + 1/\lambda_{ee}} = \frac{\lambda_{ee}/\mu_{ee}}{1 + \lambda_{ee}/\mu_{ee}},$$

customers can only access the spectrum for the remaining fraction of time, that is,

$$1 - \frac{\lambda_{ee}/\mu_{ee}}{1 + \lambda_{ee}/\mu_{ee}} = \frac{1}{1 + \lambda_{ee}/\mu_{ee}}.$$

Hence, the effective service rate μ' is smaller than μ and given by Eq. (1).

B. Validation of Delay Model with Traces of EESS Spectrum Access

To validate this delay model (i.e. Eq. 2), we leverage traces of actual EESS spectrum access. Our traces incorporate information on spectrum access at a specific location by the 14 microwave radiometers listed in Table II. The listed sensors each observe in multiple frequency bands throughout the spectrum, with all including measurements at or near 23.8 GHz. The 14 systems in Table II were selected according to existing team access to their datasets; access for an additional 14 instruments observing near 23.8 GHz was not yet acquired, thus the results to be shown represent only approximately 50% of the currently expected EESS access requests. Level 1 brightness temperature data from each sensor over the month of September 2023 was identified for situations in which the instrument's observation occurred within 100 km of latitude 42.36 deg, longitude -70.06 deg (i.e. Boston, MA). The 100 km distance is intended in part to protect the radiometer from transmissions either within the instrument antenna's main beam or from sidelobes of the antenna pattern, although more precise studies using a more accurate instrument antenna pattern model would be required to confirm the exact spatial *exclusion zone* for a given instrument. There are 783 unique satellite passes identified in this period, with mean time between arrivals of 3,387 seconds, mean access duration of 26.71 seconds, and a variance slightly greater than that of an exponential distribution. In terms of the model parameters, this yields $\lambda_{ee} = 3 \times 10^{-4}$, $\mu_{ee} = 0.04$, and $K_{ee} = 2.11$.

Satellite	Space Agency	Sensor	Source
Aqua	NASA	AMSU-A	[18]
GCOM-W	JAXA	AMSR2	[19]
GPM Core Observatory	NASA	GMI	[20]
Metop-B	EUMETSAT	AMSU-A	[21]
Metop-C	EUMETSAT	AMSU-A	[21]
NOAA-15	NOAA	AMSU-A	[22]
NOAA-18	NOAA	AMSU-A	[23]
NOAA-19	NOAA	AMSU-A	[23]
JPSS-1 (NOAA 20)	NOAA	ATMS	[24]
JPSS-2 (NOAA 21)	NOAA	ATMS	[24]
Sentinel-3A	ESA	MWR	[25]
Sentinel-3B	ESA	MWR	[25]
Sentinel-6A	EUMETSTAT	AMR-C	[26]
SNPP	NOAA	ATMS	[23]

TABLE II: EESS radiometers included in our traces.

To demonstrate the validity of the delay model, we apply a simulation in which the EESS users are generated from trace data, and commercial users are generated according to a distribution derived from studies of commercial cognitive radios under high usage [27]. The commercial users have a mean service time of 6.47 seconds ($\mu = 0.16$) distributed with a variance slightly greater than deterministic ($K = 1.49$). Customers joining the system arrive according to a (thinned) Poisson process with mean arrival rates ranging from $\lambda\phi = 0.13$ to $\lambda\phi = 0.15$ (i.e. the mean inter-arrival time ranges from 6.86 s to 7.67 s). These values yield effective traffic rates in the range $\rho' \in [0.85, 0.95]$ (i.e. resulting in a heavy traffic system while respecting the stability criteria $\rho' < 1$). As seen in Figure 3, when plotting the simulated delay times against the analytical values expected from $E[D]$, the simulated values for the customer delays fall within a 95% confidence interval of the expected value based on 30 iterations of the simulation. This shows a good match between our analytical models and the simulated model. As a result, we proceed with our analysis based on the delay model established in Section III-A.

In evaluating the trace data, we make a simplifying assumption that the presence of a radiometer results in the unavailability of the spectrum of interest. While this ignores potential re-allocations to white space (for example, the AMSU and ATMS instruments have a bandwidth of 270 MHz while others

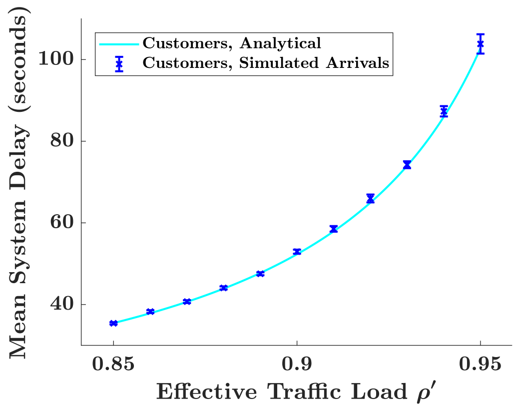

Fig. 3: Validation of delay model. The analytical curve is plotted using Equation (2). The simulated curve leverages trace data from radiometers listed in Table II and customer traffic parameters derived from previous measurement studies of commercial cognitive radios [27]. The figure shows excellent agreement between the two curves, with the analysis consistently falling within the 95% confidence interval of the simulation at all simulated values.

have a 400 MHz bandwidth), it is also important to recall that the included instruments do not represent every radiometer observing in the 23.8 GHz band. Thus, we err on the side of a conservative estimate of the rate of spectrum usage by EESS radiometers. We further note that the results shown are intended only to provide an example of the temporal properties of current EESS user spectrum access in a commonly used frequency channel, without suggesting that any particular band should be prioritized for future spectrum sharing. In addition, as the number of EESS satellites continues to grow, it should be expected that spectrum access will become more frequent, which motivates the exploration of economic impacts for a range of spectrum access parameters. We conduct such a study in Section IV-C.

C. Reward Model and Game Formulation

In defining the reward and subsequent queuing game, we leverage classical assumptions on $M/G/1$ queues in general [28], and unobservable queues in particular as customers are unable to cooperate with each other [29]. In particular, we assume that customers are homogeneous with identical reward R for successful service, that they do not balk from the queue after joining, customers are risk neutral and seek to maximize their net benefit, and users in the system have a sense of the statistical parameters of the queue despite being unable to directly observe the queue sizes. As a result, customers have two choices, to utilize the spectrum, or to not do so. A customer which does not join the queue has a reward of 0 from failing to achieve service, but a cost of 0 from avoiding the queue in the first place. Thus, to join the queue and utilize spectrum, the utility for doing so must be non-negative. We additionally assume that the stability condition $\rho' < 1$ holds even when all customers join the queue and $\phi = 1$.

As the reward R is constant, the defining element of individual utility will be the costs. WLOG, we let $R = 1$, thus *all considered costs are normalized with respect to the reward received*. From a customer point of view, the time spent waiting in the queue represents an opportunity cost, and thus we consider a cost of delay. This cost equals $C_d E[D]$, where $C_d > 0$ is the per-time unit cost imposed by the customers for delay time, and $E[D]$ is the expression for the delay from Equation (2). In addition we consider that, while we assume that the queue has a work conserving nature, customers are sensitive to preemptions and incur costs related to pausing their utilization of the available spectrum. This cost of preemption is the per-preemption cost $C_p > 0$ multiplied by the expected number of preemptions. Given that breakdowns due to arrival of EESS radiometers occur at a rate of λ_{ee}, and the service period of an individual customer is $1/\mu$ on average, the expected number of preemptions during a service period is λ_{ee}/μ.

Given this formulation, we define a *queuing utility* function $Q(\phi)$ as the individual utility of the customers opting to utilize spectrum, which is the reward minus the costs of delay and preemption:

$$Q(\phi) \triangleq 1 - \left(C_d E[D] + C_p \frac{\lambda_{ee}}{\mu} \right). \tag{3}$$

However, we must also account for the existence of a provider managing spectrum access, who charges an admission fee f to each customer joining the system. The provider incurs no other reward, nor faces ongoing costs related to access management. As a result, the provider's utility is equal to its reward, which is f multiplied by the number of customers accessing the spectrum. Conversely, the utility a customer considers when joining the queue to access spectrum equals

$$Q(\phi) - f. \tag{4}$$

It is this quantity that is the focus of our optimization efforts in the economic analysis.

IV. Economic Analysis

In this section, we present an analysis of the economic aspects of the game introduced in the previous section: the conditions under which a given fraction ϕ of customers opting to utilize the spectrum is an equilibrium state, the conditions where the equilibrium state is subsequently a socially optimal one, whether a provider profit maximization state coincides with a socially optimal state, and a sensitivity analysis derived from spectrum access traces.

A. Equilibrium Analysis

As established in Equation (4), the customers' individual utility will depend on the queuing costs and the admission fee. The fee f however is set by the provider, who is free to set it at whatever level it so chooses. An important case is one where a customer is indifferent between its options for some ϕ^*. That is, $f = Q(\phi^*)$, resulting in a utility of 0. This results in a Nash Equilibrium state where a fraction ϕ^* of customers join the queue, and the remainder do not. The provider optimizes the fee f as a function of $Q(\phi)$. To determine specific equilibrium conditions, we assert the following:

Lemma 1: Increasing the fraction of customers utilizing spectrum decreases the utility of all customers in the queue, regardless of the values of the queuing parameters for customer or EESS users.

The proof, contained in Appendix A, amounts to computing the derivative of $Q(\phi)$ and determining that it is monotone decreasing for all ϕ regardless of which values the parameters take. This customer behavior is referred to in the literature as *Avoid the Crowd* [7]. With this in mind, we define $f_0 \triangleq Q(0)$ and $f_1 \triangleq Q(1)$ respectively. Letting $\alpha \triangleq \lambda_{ee} + \mu_{ee}$ and $\beta \triangleq 2\lambda_{ee}^2 + K_{ee}\lambda_{ee}\mu + 4\lambda_{ee}\mu_{ee} + 2\mu_{ee}^2$ be notational shorthands for repeating expressions, we thus have

$$f_0 = 1 - C_d\left(\frac{\alpha}{2} + \frac{1}{\mu'}\right) - C_p\frac{\lambda_{ee}}{\mu}, \tag{5}$$

and

$$f_1 = 1 - C_d\frac{(K-2)\lambda\alpha^3 + \mu\mu_{ee}\beta}{2\mu\mu_{ee}\alpha(\lambda\alpha - \mu\mu_{ee})} - C_p\frac{\lambda_{ee}}{\mu}, \tag{6}$$

We also define the following expression for the mixed state ϕ^* which is a solution to $f = Q(\phi^*)$:

$$\phi^* \triangleq \frac{\mu\mu_{ee}\big(2\mu_{ee}\alpha(C_p\lambda_{ee} + (f-1)\mu) + C_d\beta\big)}{\lambda\alpha^2\big(2\mu_{ee}(C_p\lambda_{ee} + (f-1)\mu) - C_d(K-2)\alpha\big)}. \tag{7}$$

This leads to the following claim:

Theorem 1: Given fixed parameters, a fixed admission fee f, and f_0, f_1 as defined in Equations (5) and (6), there exists always a *unique* equilibrium state determined as follows:

1) If $f \geq f_0$, the equilibrium is $\phi = 0$ (i.e. no customer utilizes the spectrum);
2) If $f \leq f_1$, the equilibrium is $\phi = 1$ (i.e. all customers utilize the spectrum);
3) If $f_1 < f < f_0$, the equilibrium is the mixed equilibrium $\phi^* \in (0,1)$, where ϕ^* is equal to the expression in Equation (7) (i.e. a fraction ϕ^* of customers join the queue, the remaining $1-\phi^*$ do not).

Proof: From Lemma 1, $Q(\phi)$ is monotone decreasing. Thus, the maximum value of $Q(\phi)$ is f_0, and the minimum is f_1, for $\phi \in [0,1]$. Subsequently, it follows that f_0 is the lowest admission fee which ensures that no customers have incentive to join the queue; f_0 is defined in terms of the $\phi = 0$ equilibrium, thus by definition $f = f_0$ yields an equilibrium where no customers have incentive to utilize spectrum. If the admission fee is set higher than f_0, then the fee is certainly higher than any customer is willing to pay to join the queue, which has the same effect. This demonstrates the first claim.

Similarly, f_1 will be the highest admission fee ensuring that all customers have incentive to join the queue and utilize spectrum. Certainly $f = f_1$ is defined in terms of the $\phi = 1$ equilibrium; and any fee less than f_1 must also result in all customers having incentive to utilize spectrum as the provider would be charging a lower admission fee than every customer is willing to pay, thus demonstrating the second claim.

If otherwise $f_1 < f < f_0$, then it is the case that there exists some $\phi^* \in (0,1)$ such that $f = 1 - C(\phi^*)$. By definition, this is an equilibrium state. That no other $\phi \neq \phi^*$ can be an equilibrium is a consequence of the customers' behavior as demonstrated in Lemma 1. If $\phi < \phi^*$, the utility is positive, and a newly arriving commercial user has incentive to utilize the spectrum. Conversely, if $\phi > \phi^*$, the utility is now negative and therefore there is no incentive for newly arriving customers to utilize the spectrum. Therefore, the mixed equilibrium ϕ^* is unique, where ϕ^* is defined in Equation (7). ■

We conclude the equilibrium analysis by noting that no restriction was placed on the value of the admission fee f. Thus negative values are admitted, in which case f is instead an admission subsidy. While a profit maximizing provider has no incentive to set a negative admission fee, providers with other objectives may benefit from paying a subsidy (*e.g.* a public utility which has an objective of spectrum utilization inducing customers to join the queue when the reward is less than the costs of delay and preemption). As a result, this analysis is applicable to situations beyond the profit maximizing scenario.

B. Profit Maximization and Social Welfare

Under our model, a monopolistic provider controls the level at which the admission fee f is set. As such, the game is dominated by the provider's actions, notwithstanding preemptions caused by EESS users. As we consider a commercial shared spectrum setting, we assume that the provider's objective is profit maximization. Because customer arrivals form a random process, we define the profit in terms of expectation per time unit. Equilibrium states are defined in terms of the relationship between the admission fee f and the customer queuing utility $Q(\phi)$. The rate of customers who join the queue equals $\lambda\phi$. Therefore, the profit expression to optimize is

$$\mathcal{P} = \begin{cases} \lambda\phi Q(\phi) & \text{if } Q(\phi) > 0, \\ 0 & \text{if } Q(\phi) \leq 0. \end{cases} \tag{8}$$

As the provider is monopolistic, optimizing $\mathcal{P}$ potentially results in a non-optimal state in terms of the social welfare, or net utility, of all users combined. Specifically, the *Price of Anarchy (PoA)* is defined as the ratio of the optimal social welfare to the social welfare at a given equilibrium state [30]. A PoA of 1 represents a scenario where the equilibrium state is also a socially optimal one; values greater than 1 represent wasted costs from non-cooperation. However, we claim that in this setting, this is not a concern.

Theorem 2: The admission fee f which maximizes the provider profit yields the socially optimal state.

Proof: As with the profit, we consider the social welfare in terms of expected value per time unit due to the number of customers being a random variable. In this light, the utility of the λ customers depends on whether or not they utilize spectrum. The utility of the provider is simply the admission fees collected from customers opting to utilize spectrum access. This results in the following expression:

$$\lambda\left(\phi[Q(\phi)-f]+(1-\phi)0\right)+\lambda\phi f \tag{9}$$

As the payment of f from customer to provider has a net social utility of 0, and customers opting against utilizing spectrum have a utility of 0, the resulting expression simplifies to $\lambda\phi Q(\phi)$, which is the expression for $\mathcal{P}$ when $Q(\phi)>0$.

From Lemma 1, we know that $Q(\phi)$ is monotone decreasing in ϕ. Thus, the value can transition from positive to negative at most once in the interval $\phi\in[0,1]$. If it does, then there also exists some interval $(0,\phi')$ where $\lambda\phi Q(\phi)$ is positive. Thus, the maximum value of the social welfare must exist in the interval $(0,\phi')$. As the expression is equivalent to $\mathcal{P}$, this also yields the profit maximizing equilibrium from which the corresponding admission fee f is derived. Otherwise, if there is no transition between positive and negative values of $Q(\phi)$, it must be the case that $Q(\phi)<0$ for any $\phi>0$. Therefore, the social utility must also be negative in this interval. Therefore the socially optimal state is $\phi=0$, where no customers join the queue, yielding a social utility of 0. However, this is also the maximum profit a provider will realize in this scenario as no customer will utilize spectrum without being paid a subsidy to overcome the lack of incentive to join the queue.

■

As the provider profit maximization state is socially optimal, the PoA is 1 by definition. By extension, it is not necessary for a regulatory body to intervene for the purposes of inducing a socially optimal state (so long as the provider is acting in a rational manner). While such an outcome has been observed in prior studies for classical queues [29], that it continues to hold here is not obvious at first glance, due to the cost of preemptions and the generality of our model regarding the distribution of breakdown periods.

Given that computing the optimal social state and profit maximization state are equivalent, we compute the fee $f>0$ corresponding to the equilibrium $\phi^*>0$ which optimizes the profit $\mathcal{P}$. We define the following quantities, where α, β are the shorthand values defined earlier (see Table I):

$$\overline{C_d}=\frac{2\mu_{ee}\alpha(\mu-C_p\lambda_{ee})}{\beta}; \tag{10}$$

$$\underline{C_d}=\frac{2(C_p\lambda_{ee}-\mu)\mu_{ee}\alpha(\mu\mu_{ee}-\lambda\alpha)^2}{(K-2)\lambda\alpha^3(\lambda\alpha-2\mu\mu_{ee})-\mu^2\mu_{ee}^2\beta}; \tag{11}$$

$$\phi^{max}=\frac{\mu\mu_{ee}}{\lambda\alpha}-\sqrt{\frac{C_d\mu^2\mu_{ee}^2(K_{ee}\lambda_{ee}\mu+K\alpha^2)}{\lambda^2\alpha^3(C_d(K-2)\alpha-2(C_p\lambda_{ee}-\mu)\mu_{ee})}}. \tag{12}$$

The following theorem establishes the profit-maximizing fee.

Theorem 3: Let f_1 be given by Equation (6), $\overline{C_d}$, $\underline{C_d}$, and ϕ^{max} be given by Equations (10)-(12), and the queuing parameters be fixed and valid. Then the provider maximizes its profits under the following conditions:

1) All the customers join the queue (i.e., $\phi=1$) and $f=f_1$, if $0<C_p<\mu/\lambda_{ee}$ and $0<C_d\leq\underline{C_d}$.
2) A fraction $\phi=\phi^{max}$ of the customers join the queue, and $f=Q(\phi^{max})$, if $0<C_p<\mu/\lambda_{ee}$ and $\underline{C_d}<C_d<\overline{C_d}$.
3) Otherwise, the provider is unable to generate profit.

Proof: To show this result, we claim that $\mathcal{P}$ is either monotone with respect to ϕ, or unimodal with a unique maximum over the interval $\phi\in(0,1)$. We evaluate this derivative in Appendix B. Based upon this evaluation, we determine that the maximum value of $\mathcal{P}$ depends on the values of C_d and C_p and the queuing parameters:

- If $0<C_p<\mu/\lambda_{ee}$ and $0<C_d\leq\underline{C_d}$, $\mathcal{P}$ increases with respect to ϕ over the entire interval. Therefore, the maximum value of $\mathcal{P}$ occurs at $\phi=1$ with corresponding admission fee $f=f_1$ as previously defined.
- If on the other hand $0<C_p<\mu/\lambda_{ee}$ and $\underline{C_d}<C_d<\overline{C_d}$, $\mathcal{P}$ is a unimodal function increasing for $\phi\in(0,\phi^{max})$ and decreasing from $\phi\in(\phi^{max},1)$. Therefore, the maximum value of $\mathcal{P}$ occurs at $\phi=\phi^{max}$, with corresponding admission fee $f=Q(\phi^{max})$.
- Otherwise, $\mathcal{P}$ is monotone decreasing with respect to ϕ, and as $\mathcal{P}=0$ when $\phi=0$, no admission fee $f>0$ results in provider profits. Therefore, the maximum value of $\mathcal{P}$ occurs at $\phi=0$, and no customers opt to join the queue.

■

Thus, we find that while the provider profit maximization is socially optimal, in general not all customers are incentivized to join the queue in a profit maximization scenario. The costs of queuing delay and preemption must be sufficiently small relative to the queuing parameters for $\phi=1$ to be the profit maximizing equilibrium. This is of particular concern when considering scenarios in which customer traffic approaches the saturation point - the more customers present, the more likely preemptions occur despite the EESS radiometers occupying the spectrum for a small fraction of time.

C. Numerical Results

We next perform numerical analyses to illustrate our theoretical results. We utilize the EESS and commercial distributions derived in Section III-B: i.e., EESS users follow arrival and service distributions where $\lambda_{ee}=3\times10^{-4}$, $\mu_{ee}=0.04$ and $K_{ee}=2.11$; and commercial users follow arrival distribution $\lambda=0.14$, with service distribution $\mu=0.16$ and $K=1.5$, such that if $\phi=1$ the effective load is $\rho'=0.9$.

a) Evaluating the Impact of the Delay and Preemption Costs: We begin by evaluating the result of Theorem 3, using our derived parameters to visualize the relationship between the costs of delay C_d and preemption C_p and their impact on the profit maximizing equilibrium state ϕ^{max}. The results for $C_d\in(0,0.2)$ and $C_p\in\{1,10,100,1000\}$ are plotted in Figure 4. We find that so long as $C_p<\mu/\lambda_{ee}=515.33$, there will be regions where $\phi^{max}=1$ and profit is maximized when all customers join the queue. This follows from a consequence of the fact that the rate of EESS arrivals λ_{ee} is much smaller than the mean customer service length $1/\mu$. Thus, while users are sensitive to preemptions, unless the cost of preemption is 3 to 4 orders of magnitude greater than the reward, there will

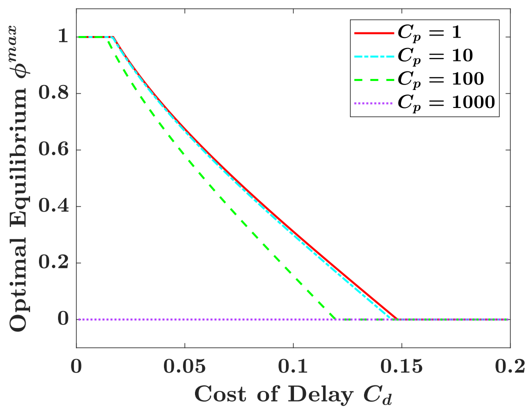

Fig. 4: Plot of the profit optimizing equilibrium ϕ^{max} resulting from cost of delay C_d in the range $(0, 0.2)$, for cost of preemption $C_p \in \{1, 10, 100, 1000\}$, using the parameters for EESS users and customers derived in Section III-B with an effective traffic load of $\rho' = 0.9$ when $\phi = 1$ (i.e. all customers join). We see that as C_d increases in this range, the profit maximizing equilibrium rapidly drops to 0; conversely, C_p must be very large relative to the reward to produce regions where $\phi^{max} = 0$ for any delay cost. These results show that customers are primarily sensitive to the delay cost.

exist scenarios where customers will opt to join the queue, as the likelihood of preemption is relatively small.

Conversely, the profit maximizing equilibrium ϕ^{max} drops to 0 rapidly as a function of C_d for fixed values of $C_p < \mu/\lambda_{ee}$, demonstrating that the customers are more sensitive to delay than preemption in this setting. Indeed, while C_p represents a per-preemption cost with a low probability of being incurred, C_d is a per-time unit delay cost incurred until the completion of service. Thus, in this scenario, values of C_d less than 20% of the reward result in scenarios where customers lack incentive to join the queue and the maximum profit is 0. Thus, customers are more sensitive to each other's traffic, than they are to the effects of preemption.

b) Evaluating the Impact of EESS Spectrum Usage Parameters: Having established sensitivity to preemption, we consider the impact of changes in spectrum usage by EESS radiometers on customer behavior. Indeed, future EESS usage requirements may entail more frequent arrival times than currently observed. This drives interest in analyzing the sensitivity of the equilibrium states as λ_{ee} varies from 3×10^{-4} and 6×10^{-4} to represent a doubling of EESS arrivals over the currently observed frequency. There are no other changes to the queuing parameters, resulting in an effective load range $\rho' \in [0.9, 0.91]$ when $\phi = 1$.

We let $C_d = 13 \times 10^{-3}$ and $C_p \in \{1, 10, 100\}$. Note that for $\lambda_{ee} = 3 \times 10^{-4}$, $\phi^{max} = 1$ for each of the selected values of C_p. Plotting the corresponding profit maximizing equilibria in Figure 5(a), we find that when C_p is sufficiently small (i.e. within one order of magnitude of the value of the reward), the profit maximizing equilibrium remains $\phi^{max} = 1$. Therefore, despite the increase in EESS traffic, the relatively low sensitivity to preemption results in profit maximization still occurring when all customers join the queue. Conversely, if the cost of preemption is two orders of magnitude greater than the reward (e.g. $C_p = 100$), then situations where ϕ^{max} is a mixed equilibrium state arise. Specifically, here we find that $\lambda_{ee} > 3.49 \times 10^{-4}$ results in $\phi^{max} < 1$. This EESS arrival rate represents one arrival every 2,865 seconds, or a 16% increase over the observed rate from our trace data. Thus, if customers value preemption is sufficiently high, a marginal increase in EESS traffic may result in some customers not wanting to join the queue and utilize the available spectrum. However, even if λ_{ee} doubles, the corresponding $\phi^{max} = 0.93$, meaning that only 7% of the customers do not join the queue. Thus, while profit maximization does not occur when all customers join the queue, the vast majority of customers will still opt to do so in this scenario.

In Figure 5(b), we plot the corresponding provider profits $\mathcal{P}$ for our scenarios. For $C_p = 1$ and $C_p = 10$, we find that an increase in EESS traffic has a limited impact on provider profits. However, in the case $C_p = 100$, the realized profit decreases with the increased EESS traffic; while the likelihood of preemption is still relatively low, the increased sensitivity to preemption forces the provider to charge a lower fee to convince customers to join the queue. As EESS traffic doubles, the profit decreases by 40%, despite only 7% fewer customers joining the queue. Yet, the doubling of EESS arrivals only decreases the available white-space for customer transmissions from 99.2% to 98.4%. Thus, marginal decreases in available spectrum can result in profit decreases which are much larger. Therefore, a high sensitivity to preemption could be a concern as EESS usage of available spectrum changes, despite customer behavior generally being dominated by sensitivity to delay from other customers entering the system, as shown in the previous example.

V. Conclusions

In this work we propose a spectrum sharing framework on frequency bands utilized by the Earth Exploration Satellite-Service, which comprises passive radiometers in orbit and thus individual radiometers only requiring access to spectrum for a brief period as they pass overhead in a given location. Leveraging concepts from queuing theory and game theory, we develop an economic model for spectrum sharing between EESS users and a commercial tier. Utilizing traces of EESS data from the Boston area during September 2023, we demonstrate that commercial user delay can be modeled using an $M/G/1$ queue with *server breakdowns*, where the breakdown periods caused by EESS arrivals follow a general distribution. Accordingly, we develop a queuing game that captures the customer rewards gained by spectrum access, as well as costs proportional to the delay in the queue and frequency of preemptions under service. We fully solve the game as a function of the system parameters, including providing a closed-form expression for the Nash equilibrium, which is also proven to be unique. We further determine the regime

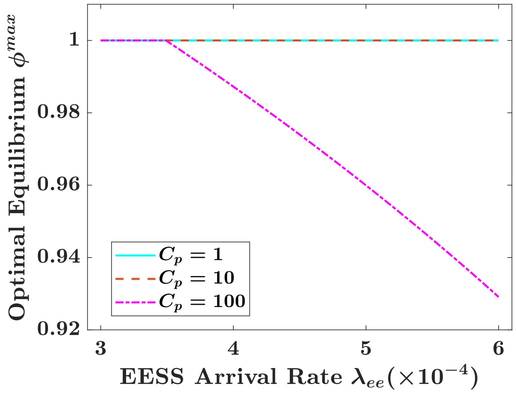

(a) Optimal equilibrium vs. EESS arrival rate

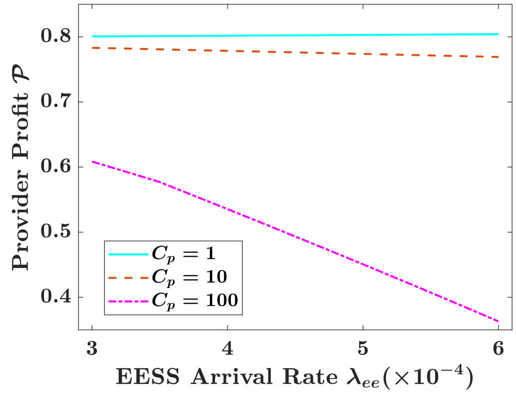

(b) Maximum profit vs. EESS arrival rate

Fig. 5: Plots of the profit maximizing equilibrium (left) and corresponding provider profit (right) as a function of EESS user arrival rate, with customer queue statistics and EESS service parameters derived from Section III-B, and costs of delay and preemption $C_d = 13 \times 10^{-3}$ and $C_p \in \{1, 10, 100\}$, respectively. We find that when the cost of preemption is not too high (i.e. $C_P \leq 10$), increase in EESS traffic does not affect the optimal equilibrium (i.e., $\phi^{max} = 1$, throughout) and has a limited impact on the provider's profit. However, when $C_p = 100$, we see that increases in EESS traffic result in the profit maximizing equilibrium becoming a mixed state (i.e, $\phi^{max} < 1$). In this case, the decreasing fraction of customers joining the queue results in profits decreasing at a fast clip.

of parameters under which a commercial provider is ensured to make profit and derive the profit-maximizing fee.

An important insight from the analysis is there is no requirement for external intervention to induce a socially optimal state, because the profit maximization and social welfare optimization objectives coincide (i.e., the PoA equals 1). This reduces the regulatory overhead required to administer spectrum access on EESS bands. Further, our EESS trace data suggests that 99.2% of spectrum capacity is available on EESS bands, thus making such frequencies desirable for commercial use as the probability of EESS preemption is low. Indeed, generally customers are far more sensitive to delay than preemption to the point where the cost of preemptions must be one hundred times greater than the reward of service to have an appreciable impact on customer decision-making. In such a scenario, increases in EESS arrivals can result in provider profit decreases of 40% compared to prior EESS usage levels, despite only a 7% decrease in the fraction of customers willing to utilize the spectrum and a 0.8% decrease in spectrum availability for customers. Thus, when planning spectrum access policies, customer sensitivity to preemption must be carefully accounted for. Nevertheless, even in this case, we find that there are significant societal benefits to such a spectrum sharing paradigm, as a large fraction of potential customers would be able to access spectrum and commercial service would be profitable.

Future work includes further refinement of our model through undertaking precise measurements of antenna patterns to confirm the nature of each instrument's *exclusion zone*, in order to refine estimates of antenna usage for spectrum planning purposes. In addition, analysis of additional EESS spectrum bands is required to determine which bands should be prioritized for spectrum sharing, given availability for commercial use balanced against customer tolerance for preemption and frequency range requirements of commercial applications.

Acknowledgment

This research was supported in part by the NSF under grants AST-2229103 and AST-2229104.

References

[1] National Research Council Report, *Spectrum management for science in the 21st century*, 2010.

[2] ITU-R, "Performance and interference criteria for satellite passive remote sensing RS Series Remote sensing systems," ITU-R Recommendation RS.2017, Tech. Rep., 2012. [Online]. Available: http://www.itu.int/ITU-R/go/patents/en

[3] A. Lopatka, "Fifth-generation broadband wireless threatens weather forecasting," *Physics Today*, vol. 72, no. 8, pp. 24–26, aug 2019. [Online]. Available: http://physicstoday.scitation.org/doi/10.1063/PT.3.4267

[4] A. Witze, "Global 5G wireless networks threaten weather forecasts," *Nature*, vol. 569, no. 7754, pp. 17–19, May 2019.

[5] D. W. Draper and E. F. Stocker, "A comparison of radio frequency interference within and outside of allocated passive earth exploration bands at 10.65 GHz and 18.7 GHz using the GPM microwave imager and windsat," *International Geoscience and Remote Sensing Symposium (IGARSS)*, vol. 2017-July, pp. 2731–2733, 2017.

[6] E. Koutsoupias and C. Papadimitriou, "Worst-case equilibria," in *Annual symposium on theoretical aspects of computer science*. Springer, 1999, pp. 404–413.

[7] R. Hassin and M. Haviv, *To Queue or Not to Queue: Equilibrium Behavior in Queueing Systems*, ser. International Series in Operations Research & Management Science. Boston, MA, USA: Springer US, 2003, vol. 59.

[8] R. Hassin, *Rational Queueing*. CRC press, 2016.

[9] J. Chamberlain and D. Starobinski, "Social welfare and price of anarchy in preemptive priority queues," *Operations Research Letters*, vol. 48, no. 4, pp. 530–533, 2020.

[10] ——, “Strategic revenue management of preemptive versus non-preemptive queues,” *Operations Research Letters*, vol. 49, no. 2, pp. 184–187, 2021.
[11] B. Avi-Itzhak and P. Naor, “Some queuing problems with the service station subject to breakdown,” *Operations Research*, vol. 11, no. 3, pp. 303–320, 1963.
[12] S. M. Ross, *Introduction to probability models*, 11th ed. Academic press, 2014.
[13] C. T. Do, N. H. Tran, Z. Han, L. B. Le, S. Lee, and C. S. Hong, “Optimal pricing for duopoly in cognitive radio networks: Cooperate or not cooperate?” *IEEE Transactions on Wireless Communications*, vol. 13, no. 5, pp. 2574–2587, May 2014.
[14] Federal Communications Commission, “3.5 GHz Band Overview,” Accessed: June 23, 2021. [Online]. Available: https://www.fcc.gov/wireless/bureau-divisions/mobility-division/35-ghz-band/35-ghz-band-overview
[15] E. Eichen, “Performance of real-time geospatial spectrum sharing (rgss) between 5g communication networks and earth exploration satellite services,” in *2021 IEEE International Symposium on Dynamic Spectrum Access Networks (DySPAN)*, Dec 2021, pp. 73–79.
[16] R. Conway, W. Maxwell, and L. Miller, *Theory of Scheduling*. Reading, MA, USA: Addison-Wesley, 1967.
[17] D. Willkomm, S. Machiraju, J. Bolot, and A. Wolisz, “Primary user behavior in cellular networks and implications for dynamic spectrum access,” *IEEE Communications Magazine*, vol. 47, no. 3, pp. 88–95, 2009.
[18] “AIRS/Aqua L1B AMSU (A1/A2) geolocated and calibrated brightness temperatures V005,” Accessed: November 20, 2023. [Online]. Available: https://disc.gsfc.nasa.gov/datasets/AIRABRAD_005/summary
[19] “GCOM-W AMSR-2 Level 1 Brightness Temperature Data,” Accessed: November 20, 2023. [Online]. Available: https://gportal.jaxa.jp/gpr/search?tab=1
[20] “GPM GMI Brightness Temperatures L1B 1.5 hours 13 km V07,” Accessed: November 20, 2023. [Online]. Available: https://disc.gsfc.nasa.gov/datasets/GPM_1BGMI_07/summary
[21] “AMSU-A Level 1B Data - Metop,” Accessed: November 20, 2023. [Online]. Available: https://data.eumetsat.int/product/EO:EUM:DAT:METOP:AMSUL1
[22] “MSU/AMSU-A Brightness Temperature - NOAA Climate Data Record (CDR) ,” Accessed: November 20, 2023. [Online]. Available: https://www.ncei.noaa.gov/has/HAS.FileAppRouter?datasetname=NSTAR_FCDR\&subqueryby=STATION\&applname=\&outdest=FILE
[23] “Index of /data/amsu-a-brightness-temperature/access,” Accessed: November 20, 2023. [Online]. Available: https://www.ncei.noaa.gov/data/amsu-a-brightness-temperature/access
[24] “NOAA JPSS Advanced Technology Microwave Sounder (ATMS) Temperature Data Record (TDR) from IDPS,” Accessed: November 20, 2023. [Online]. Available: https://www.ncei.noaa.gov/access/metadata/landing-page/bin/iso?id=gov.noaa.ncdc:C01426
[25] “Sentinel-3 SRAL Level 2 Data,” Accessed: November 20, 2023. [Online]. Available: https://documentation.dataspace.copernicus.eu/Data/Sentinel3.html\#sentinel-3-sral-level-2
[26] “Climate-quality Advanced Microwave Radiometer Level 2 Products in NRT - Sentinel-6,” Accessed November 20, 2023. [Online]. Available: https://navigator.eumetsat.int/product/EO:EUM:DAT:0146
[27] M. Lopez-Benitez and F. Casadevall, “Time-dimension models of spectrum usage for the analysis, design, and simulation of cognitive radio networks,” *IEEE transactions on vehicular technology*, vol. 62, no. 5, pp. 2091–2104, 2013.
[28] P. Naor, “The regulation of queue size by levying tolls,” *Econometrica: journal of the Econometric Society*, pp. 15–24, 1969.
[29] N. M. Edelson and D. K. Hilderbrand, “Congestion tolls for poisson queuing processes,” *Econometrica: Journal of the Econometric Society*, pp. 81–92, 1975.
[30] G. Gilboa-Freedman, R. Hassin, and Y. Kerner, “The Price of Anarchy in the Markovian Single Server Queue,” *IEEE Transactions on Automatic Control*, vol. 59, no. 2, pp. 455–459, 2014.

Appendix A
Proof of Lemma 1

To prove the claim in Lemma 1, we assert that even a marginal increase in the fraction of customers entering the queue to utilize spectrum reduces the utility of all customers electing to do so. Conversely, a decrease in the fraction of customers joining the queue increases the utility of customers who opt to join. The net utility for an individual customer is given by $Q(\phi)-f$; f is set by the provider, who optimizes the fee in terms of $Q(\phi)$ to achieve a targeted equilibrium state. Therefore, $Q(\phi)$ is the quantity to consider when evaluating customer behavior as the admission fee varies. Applying Equations (2) and (3) and the notational shorthand $\alpha = \lambda_{ee} + \mu_{ee}$, $Q(\phi)$ is expressed as

$$1 - \left[C_d \left(\frac{K_{ee}\lambda\mu^2\mu_{ee} + K\lambda\alpha\phi}{2\mu\mu_{ee}\alpha(\mu\mu_{ee} - \lambda\alpha\phi)} + \frac{\alpha}{\mu\mu_{ee}} \right) + C_p \frac{\lambda_{ee}}{\mu} \right].$$

The only term containing a ϕ is a quotient, however the restrictions $\phi \in [0,1]$ and the stability assumption $\rho' < 1$ imply that the denominator must be greater than 0. By inspection, we conclude the expression is continuous and differentiable over the interval $\phi \in [0,1]$. Computing the derivative yields:

$$-\frac{C_d \left(K_{ee}\lambda_{ee}\mu + K\alpha^2 \right)}{2(\mu\mu_{ee} - \lambda\alpha\phi)^2}.$$

Given that the individual parameters must be positive by their definitions, and the previously stated stability assumption and restricted domain of ϕ, we conclude the derivative is negative for all $\phi \in [0,1]$. Therefore, as a function of ϕ, the net utility is monotone decreasing, the physical interpretation being that of the Lemma's claim: increasing the fraction of customers in the queue decreases the utility for all customers.

Appendix B
Behavior of Provider Profit $\mathcal{P}$ as a Function of ϕ

In Theorem 3, the proof depends on evaluating the derivative of $\mathcal{P}$ with respect to ϕ to determine the behavior of $\mathcal{P}$ as ϕ changes and in turn determine where the maximum value exists on the interval $\phi \in [0,1]$. We assert that as $\mathcal{P} = \lambda\phi Q(\phi)$ and $Q(\phi)$ was previously determined to be differentiable in Lemma 1, so too is $\mathcal{P}$ as a function of ϕ. Computing said derivative yields

$$\frac{\lambda(\mu - C_p\lambda_{ee})}{\mu} - C_d\lambda \left(\frac{\mu\mu_{ee}\beta}{2\alpha(\mu\mu_{ee} - \lambda\alpha\phi)^2} + \frac{(K-2)\lambda\alpha^2\phi(2\mu\mu_{ee} + \lambda\alpha\phi)}{2\mu\mu_{ee}(\mu\mu_{ee} - \lambda\alpha\phi)^2} \right).$$

Evaluating this quantity over $\phi \in (0,1)$ given the restrictions on the parameters, we find that to be positive requires $C_p < \mu/\lambda_{ee}$. There are two additional sub cases based on the value of C_d. If $C_p \leq \underline{C_p}$ as defined in Equation (11), the derivative is positive for all $\phi \in (0,1)$. Otherwise, if $\underline{C_p} < C_p < \overline{C_p}$, for $\overline{C_p}$ as defined in Equation (10), the derivative will be positive in the interval $(0, \phi^{max})$ as defined in Equation (12). Otherwise, the derivative is negative over the interval $\phi \in (0,1)$. Thus, we establish bounds for the maximum profit and its associated equilibrium, enabling the completion of the proof of Theorem 3.